Extensive remodeling of a cyanobacterial photosynthetic apparatus in far-red light

Authors: Fei Gan, Shuyi Zhang, Nathan C. Rockwell, Shelley S. Martin, J. Clark Lagarias, and Donald A. Bryant

Gan, Fei, Shuyi Zhang, Nathan C. Rockwell, Shelley S. Martin, J. Clark Lagarias, and Donald A. Bryant. "Extensive remodeling of a cyanobacterial photosynthetic apparatus in far-red light." Science (2014): 1256963. http://dx.doi.org/10.1126/science.1256963

Extensive remodeling of a cyanobacterial photosynthetic apparatus in far-red light

Fei Gan, Shuyi Zhang, Donald A. Bryant: Department of Biochemistry and Molecular Biology, The Pennsylvania State University, University Park, PA
Nathan C. Rockwell, Shelley S. Martin, J. Clark Lagarias: Department of Molecular and Cellular Biology, University of California, Davis, CA 95616, USA.
Donald A. Bryant: Department of Chemistry and Biochemistry, Montana State University, Bozeman, MT 59717 USA.

Abstract

Cyanobacteria are unique among bacteria in performing oxygenic photosynthesis, often together with nitrogen fixation and, thus, are major primary producers in many ecosystems. The cyanobacterium, *Leptolyngbya* sp. strain JSC-1, exhibits an extensive photoacclimative response to growth in far-red light that includes the synthesis of chlorophylls *d* and *f*. During far-red acclimation, transcript levels increase ≥2-fold for ~900 genes and decrease ≥2-fold for ~2000 genes. Core subunits of photosystem I, photosystem II, and phycobilisomes are replaced by proteins encoded in a 21-gene cluster that includes a knotless red/far-red phytochrome and two response regulators. This acclimative response enhances light harvesting for wavelengths complementary to the growth light (λ = 700 to 750 nm) and enhances oxygen evolution in far-red light.

Cyanobacteria are unique among bacteria in performing oxygenic photo-synthesis and are ecologically important primary producers (*1*). Marine cyanobacteria, mostly *Prochlorococcus*, *Synechococcus*, and *Tricho-desmium* species, account for >25% of the net primary productivity in oceans, and terrestrial cyanobacteria also contribute significantly to global photosynthesis (*2*, *3*). The estimated cyanobacterial biomass in terrestrial, endolithic, and freshwater lake ecosystems is ~2.5-fold lower than that in oceans, but this estimate would increase if polar and subarc-tic soils, topsoils in sub-humid climates, and shallow marine and fresh-water benthic environments were included (*2*). Because approximately equal solar irradiance reaches Earth's surface in the wavelength ranges 600-700 nm and 700-800 nm (18.4% versus 14.9% of the total irradiance between 400 and 1100 nm), the capacity to use far-red light to perform oxygenic photosynthesis in terrestrial niches could thus have important consequences in natural and engineered systems.

Cyanobacteria mainly use three large, multisubunit complexes to harvest and convert light into stable, energy-rich compounds: Photosystem (PS) I, PS II, and phycobilisomes (PBS) (*1*, *4*–*7*). Cyanobacteria have evolved many mechanisms to maximize their photosynthetic efficiency in response to the incident irradiation. Examples include adjusting the total cellular chlorophyll (Chl) content and the ratio of PS II to PS I ("intensity adaptation") (*8*), state transitions that redistribute light energy transfer from PBS to PS I and PS II (*9*, *10*), and non-photochemical quenching by orange carotenoid-binding protein (*11*). Although cyanobacteria were once thought to have simple pigmentation (Chl *a*, β-carotene, and phycobiliproteins), it is now recognized that some cyanobacteria synthesize Chls *b*, *d* or *f* (*12*), many functionally distinct carotenoids (*13*), and a spectroscopically diverse phycobiliproteins (*7*). Limitation for iron and other nutrients causes changes in light-harvesting proteins (*14*–*16*).

One of the best-characterized acclimative responses in cyanobacteria, Complementary Chromatic Acclimation (CCA; formerly "Adaptation"), was discovered more than 100 years ago. Gaidukov (*17*, *18*) observed that Oscillatoria sancta is reddish brown when grown in green light but blue-green when grown in red light, and he correctly surmised that the color differences were due to altered pigment synthesis (fig. S1). CCA results from compositional remodeling of the peripheral rods of PBS (19, 20) and occurs through transcriptional and post-transcriptional regulation of specific phycobiliprotein genes. Genes encoding phycoerythrin and its associated bilin reductases, bilin lyases, and linker proteins are expressed in cells grown in green light, while those for "inducible" phycocyanin and associated proteins are expressed in cells grown in red light (19–22). Central regulatory elements controlling CCA include two response regulators (RcaF and RcaC) and a phytochrome-related sensor histidine kinase, RcaE (19, 20, 23). Because PBS are primarily but not exclusively asso-ciated with energy transfer to PS II (9, 10), CCA enhances the overall rate of photosynthesis when the incident irradiation is complementary to cell coloration.

Using a systems biology approach,including genome sequencing, comparative genomics, transcription profiling (RNA-Seq), biochemical and spectroscopic analyses, and proteomics, we show that *Leptolyngbya* sp. strain JSC-1 (hereafter JSC-1) (*24*) remodels its photosynthetic apparatus in response to far-red illumination. These changes are probably controlled by a red/far-red responsive phytochrome. JSC-1 specifically synthesizes both Chl *d* and Chl *f*, in addition to Chl *a*, when cells are grown with light wavelengths ≥700 nm. *Halomicronema hongdechloris*, a cyanobacterium isolated from a stromatolite from Shark Bay, Austral-ia, also synthesizes Chl *f* when cells are grown in far-red light (*25*, *26*). However, JSC-1 additionally undergoes an extensive acclimative re-sponse, in which the expression of ≥40% of the genome changes more than two-fold after a shift from white light to far-red light. The resulting changes in gene expression lead to the replacement of most of the core proteins of PS I and PS II and to structural remodeling of PBS core sub-structures. We named this global acclimation response "Far-Red Light Photo-acclimation" (FaRLiP), and we show here that FaRLiP significantly improves photosynthetic performance in far-red light.

The JSC-1 genome has a 21-gene cluster that encodes paralogs of most of the core subunits of PS I, PS II, and PBS (fig. S2). Similar clusters occur in 12 other cyanobacteria, including members of all five sections of the taxon *Cyanobacteria* (*27*) (fig. S3). All but one of these clusters contain six genes encoding subunits of PS I: *psaA2, psaB2, psaL2, psaI2, psaF2,* and *psaJ2* (in the remaining strain, *psaF2-psaJ2* are adjacent and probably cotranscribed with *psaB3*). The *psaA2* and *psaB2* genes are significantly diverged from the *psaA1* (~77% identity, 85% similarity), *psaB1* (85% identity, 92% similarity) and *psaB3* (82% identity, 90% similarity) genes, respectively. The other *psa* genes in this cluster (*psaL2, psaI2, psaF2,* and *psaJ2*) are similarly distantly related to paralogous *psa* genes (*psaL1, psaL3, psaI1, psaF1, psaJ1*) encoded elsewhere in the genome (see table S1 for a list of genes for subunits of PS I, PS II, and PBS and related proteins). Transcriptional analyses (ta-bles S1 and S2) showed that the *psaA2B2L2I2F2J2* genes are not expressed in cells grown under standard growth conditions for many

cyanobacteria (*28*). Interestingly, this locus also includes genes for a knotless phytochrome (*rfpA*), a DNA-binding response regulator (*rfpB*) with two CheY receiver domains and a winged-helix DNA binding domain, and a *cheY*-like gene (*rfpC*), which form an apparent operon upstream from *psbA4* (fig. S2; *rfp* = Regulator of Far-red Photoacclimation). Phytochromes are widespread red/far-red photoreceptors (*29*), but orthologs of *rfpA* only occur in 12 other cyanobacteria, within photosynthesis gene clusters similar to that in JSC-1 (fig. S3). Based upon phylogenetic analyses and conserved domain architecture, these photoreceptors form a distinctive subfamily among knotless phytochromes (Fig. 1). On the basis of these observations and biochemical studies described below, we hypothesize that the RfpA photoreceptor controls gene expression from this cluster.

Expression of *rfpA* or its GAF domain in an engineered, phycocyanobilin-producing strain of *Escherichia coli* (*28*, *30*) yielded red/far-red reversible proteins with nearly identical photochemical properties (figs. S5 and S6A). Like the knotless phytochrome NpR4776 from *Nostoc punctiforme*, recombinant RfpA-GAF holoprotein photoconverts between red-absorbing (P_r) and far-red-absorbing (P_{fr}) species under respective far-red or red illumination (fig. S6A). The P_r form of cyanobacterial phytochromes is initially synthesized in vivo (*31*, *32*). RfpA is converted to the P_{fr} form under a broad range of light wavelengths, but only far-red light ($\lambda \geq 700$ nm) specifically regenerates the P_r form (fig. S6B). Because genetic tools are not available to produce an *rfpA* mutant in JSC-1, the postulated role of RfpA in sensing far-red light and controlling expression of the 21-gene photosynthesis gene cluster cannot be verified by reverse genetics. However, RfpA specifically senses far-red light, exhibits higher transcript abundance in cells grown in far-red light, and is uniquely co-localized with genes that are only expressed in far-red light (figs. S2, S3, S5, and S6 and table S1). The JSC-1 genome contains other phytochromes and related photosensors, but transcript levels only increase in far-red light for the knotted phytochrome CYJSC1_DRAFT_40400 (Fig. 1 and table S2). *Calothrix* sp. PCC 7507 and *Synechococcus* sp. PCC 7335 have RfpA orthologs (fig. S3) but lack Cph1 orthologs. Thus, the distribution and photochemical properties of RfpA strongly support our proposal that RfpA controls the expression of the 21-gene cluster.

To examine the photobiology more closely, JSC-1 cells were grown under six light conditions (*28*): white fluorescent light (WL), green-filtered fluorescent light (GL), red-filtered fluorescent light (RL), 645-nm or 710-nm light provided by LEDs, and far-red light (FR) produced from filtered tungsten light ($\lambda > 690$ nm) (see fig. S7). The absorption spectra of cells grown in 710-nm light and FR (Fig. 2) showed that they had gained absorption at ~700–750 nm (λ_{max} ~706 nm) that was not present in cells grown in WL, GL, or 645-nm light. Low-temperature fluorescence emission spectra at 77 K (fig. S8) of cells grown under the latter three conditions had emission maxima at 683 nm and 695 from PS II and a strong emission maximum at 725 nm from PS I. These spectra are typical of those for cells synthesizing Chl *a* and having a relatively high PS I:PS II ratio (*24*). JSC-1 cells grown in 710-nm light or FR have weak fluorescence emission at 683, 695 and 717 nm and strong emission at 745 nm, resembling cells synthesizing Chl *f* (*25*, *26*).

Pigments extracted from these cells were subjected to reversed-phase HPLC chromatography. Only Chl *a* (figs. S9 and S10, peak 3) and carotenoids were observed in pigment extracts from cells grown in WL or 645-nm light. Cells grown in FR or 710-nm light still produced Chl *a* as the major Chl, but they also synthesized a pigment with an absorption spectrum identical to that of Chl *f* (figs. S9 and S10, peak 2) (*33*, *34*). This pigment was confirmed to be Chl *f* by converting it to the corresponding pheophytin by removing the Mg^{2+} ion (figs. S11 and S12) and subsequent mass spectrometry (figs. S13 and S14). Another Chl, which was slightly more hydrophilic than Chl *f* (figs. S9 and S10, peak 1), was also detected. The absorption properties (figs. S10 and S12) of this Chl, and MS and MS-MS analyses (figs. S15 and S16) of the corresponding pheophytin, showed that it was Chl *d* (*33*, *34*). Therefore, JSC-1 synthesizes three Chls: Chl *a*, Chl *d*, and Chl *f*.

Preliminary RT-PCR experiments confirmed that genes of the *psa2* operon (fig. S2) are transcribed in cells grown in FR (table S2). Cells were therefore grown in WL, transferred to FR for 24 hours, and transcription profiling (RNA-Seq) was performed (*28*). Transcript levels for the photosynthesis-related genes in the 21-gene cluster (fig. S2) increased from 3–fold to 278–fold in cells grown in FR (Fig. 3 and table S1), and transcript levels increased ≥2-fold for ~900 genes (table S2). Transcript levels decreased ≥2-fold for ~2000 genes in FR (table S2), including most of the paralogous genes encoding core subunits of photosynthetic complexes (Fig. 3 and table S1). The transcriptional changes during acclimation to FR are surprisingly extensive and exceed those for heterocyst (1036 genes) or hormogonia (1762 genes) differentiation in *Nostoc punctiforme* (*35*).

The transcription profiling data indicated that most core polypeptides of PS I, PS II, and PBS should be replaced by products of the 21-gene cluster when cells are grown in FR. To verify that this was the case, we analyzed the proteins of photosynthetic complexes isolated from JSC-1 cells grown in WL, FR, 645-nm light, and 710-nm light. Fractions enriched in PS I and/or PS II were isolated on sucrose gradients after solubilization of thylakoid membranes with *n*-dodecyl-β–D-maltoside (Fig. 4A). For JSC-1 cells grown in WL and 645-nm light, two green fractions were observed: an upper green fraction containing PS I monomers and PS II dimers, and a lower green fraction containing PS I trimers (Fig. 4A). Gradients prepared with solubilized membranes from JSC-1 cells grown in FR and 710-nm light differed dramatically. No PS I trimers were observed, and only a single fraction containing PS I monomers and PS II dimers was observed (Fig. 4A). The complexes derived from cells grown in WL or 645-nm light had absorption (Fig. 4B) and 77K fluorescence emission maxima (Fig. 4C) expected for PS I (725 nm) and PS II (685 and 695 nm) complexes containing Chl *a*. However, complexes isolated from cells grown in FR and 710-nm light had additional absorption features at ~720 nm (Fig. 4B) and had fluorescence emission maxima at 745 nm (Fig. 4C). These spectra demonstrate that both PS I and PS II complexes of cells grown in FR and 710-nm light contain Chl *f*.

Proteins associated with isolated photosynthetic complexes were analyzed by trypsin digestion and mass spectrometry of the resulting peptides (table S1). This analysis demonstrated that the core polypeptides comprising complexes from cells grown in FR and 710-nm light were the products of those genes whose transcript levels strongly increased in cells grown under FR (e.g., *psaA2, psaB2, psaL2, psaF2; psbB2, psbC3, psbD3, psbA3, psbA4, psbH2*) (table S1). In contrast, the core proteins in complexes from cells grown in WL or 645-nm light instead contained products of paralogous genes with lowered transcript levels under FR (e.g., *psaA1, psaB1, psbB1, apcE1*) (Fig. 3, table S1). Thus, the proteins comprising PS I and PS II differed in response to the growth light conditions.

PBS were isolated from cells grown in 645-nm and 710-nm light to assess whether absorption differences accompanied polypeptide replacement in FR (Fig. 5A). PBS isolated from cells grown in 710-nm light have an absorbance feature at 708 nm that is correlated with a low-temperature fluorescence emission peak at 723 nm, but PBS isolated from cells grown in 645-nm light lack these features (Fig. 5B). The 708-nm absorption band is red-shifted nearly 40 nm compared to allophycocyanin-B (λ_{max} = 670 nm), previously the most red-shifted absorption for characterized native phycobiliproteins (*36*). After denaturation of PBS proteins in 8.0 M urea at pH 3 (fig. S17), only phycocyanobilin and phycoerythrobilin were detected (*37*), suggesting that the long-wavelength absorption arises from phycocyanobilin and not from a new bilin chromophore. Strikingly, even PBS ultrastructure changes in cells grown in FR. The ApcE1 core linker phycobiliprotein expressed in WL

and 645-nm light has four linker-repeat (REP) domains and thus is predicted to assemble PBS with "pentacylindrical" core substructures (*7*, *38*) (Fig. 6A, top). ApcE1 has a highly conserved cysteine residue at position 197 that ligates a phycocyanobilin chromophore via a thioether linkage (*7*). ApcE2, the core linker phycobiliprotein synthesized in FR, has only two REP domains and thus is predicted to produce PBS with only two core cylinders (*7*, *38*) (Fig. 6A, bottom). ApcE2 has no cysteine residues in its N-terminal phycobiliprotein domain; thus, ApcE2 should bind phycocyanobilin noncovalently. Noncovalently bound phycocyanobilin would have one additional conjugated double bond, which should shift the absorption and fluorescence emission of ApcE2 to longer wavelength, as shown by site-directed mutagenesis of *apcE* in *Synechococcus* sp. PCC 7002 (*39*). Such changes could significantly modify the energy transfer pathway(s) and efficiency in the cores of PBS in cells grown in FR. These observations raise the possibility that other core PBS subunits (ApcA2, ApcB2, ApcD3, ApcD4) could also bind phycocyanobilin noncovalently to increase absorption of FR light ($\lambda \geq 700$ nm).

JSC-1 thus remodels its photosynthetic apparatus during FaRLiP by synthesizing Chl *d* and *f*, replacing the core subunits of PS I and PS II, and modifying the proteins of the PBS core as summarized in Fig. 6. Analogously to CCA, these changes produce photosynthetic complexes with absorption that is complementary to the incident irradiation between 700 and 750 nm. Additionally, JSC-1 alters relative transcript levels for >40% of the JSC-1 genome, leading to extensive modification of cellular metabolism (table S2). The transcription changes and global replacement of core components of PS I, PS II, and PBS during FaRLiP are distinct from the incorporation of PsbA variants in PS II complexes of *Synechocystis* sp. PC 6803 and other cyanobacteria in response to high light intensity or anoxic conditions (*40*) and from reported transcription changes for *psbD3* and *psbE2* of *Acaryochloris marina* cells grown in FR or WL at very low irradiance (*41*).

There is no overlap between the structural remodeling of photosynthetic complexes that occurs during CCA and FaRLiP, and interestingly, JSC-1 performs both acclimation responses (see fig. S1) (*24*). We assume that PS I, PS II, and PBS subunits produced during FaRLiP have adapted through evolution to perform photosynthesis more efficiently when some Chl *a* molecules are replaced by Chl *f* (and Chl *d*) in cells growing in FR. Indeed, JSC-1 cells that have acclimated to 710-nm light have 40% greater oxygen evolution with far-red actinic light than cells acclimated to 645-nm light, although the two types of cells have identical light saturation behavior when the actinic light is WL (fig. S18). This enhanced photosynthetic performance in FR would be ecologically significant whenever cells grow in light that is strongly filtered by Chl *a* absorbance—for example, in mats, stromatolites, cyanobacterial blooms, or in the shade of plants. FaRLiP should also benefit organisms living in sandy soils, because far-red light penetrates deeper than visible wavelengths (*42*). The 730 nm: 650 nm ratio shifts from ~0.84 at the soil surface to 2.8 at a depth of 6 mm (*43*), and this could be further enhanced by Chl *a* absorption filtering. Thus, FaRLiP could have a significant impact on cyanobacterial photosynthesis in soil crusts (two organisms in fig. S3 are soil isolates).

Our results show that it is possible for cyanobacteria to retain paralogous copies of genes for functionally specialized photochemical reaction centers. This observation has important implications for the evolution of type-1 and type-2 reaction centers during the evolution of photosynthesis as well as for the extension of Chl biosynthetic pathways (*44*). If type-1 reaction centers evolved first, a likely mechanism for the origin of type-2 reaction centers was gene duplication and functional divergence (*44*–*46*). As shown in this study, functionally distinctive and divergent PS I and PS II reaction centers are formed in strain JSC-1 during growth in FR. Finally, our findings could have important implications for introducing the capacity to utilize FR into plants.

References and Notes

1. D. A. Bryant, N.-U. Frigaard, Prokaryotic photosynthesis and phototrophy illuminated. *Trends Microbiol.* **14**, 488–496 (2006). Medline doi:10.1016/j.tim.2006.09.001
2. F. Garcia-Pichel, J. Belnap, S. Neuer, F. Schanz, Estimates of global cyanobacterial biomass and its distribution. *Algol. Stud.* **109**, 213–227 (2003). doi:10.1127/1864-1318/2003/0109-0213
3. P. Flombaum, J. L. Gallegos, R. A. Gordillo, J. Rincón, L. L. Zabala, N. Jiao, D. M. Karl, W. K. Li, M. W. Lomas, D. Veneziano, C. S. Vera, J. A. Vrugt, A. C. Martiny, Present and future global distributions of the marine cyanobacteria *Prochlorococcus* and *Synechococcus*. *Proc. Natl. Acad. Sci. U.S.A.* **110**, 9824–9829 (2013). Medline doi:10.1073/pnas.1307701110
4. D. A. Bryant, Ed., *The Molecular Biology of Cyanobacteria*, vol. 1 of *Advances in Photosynthesis and Respiration* (Kluwer Academic, Dordrecht, Netherlands, 1994).
5. I. Grotjohann, P. Fromme, Structure of cyanobacterial photosystem I. *Photosynth. Res.* **85**, 51–72 (2005). Medline doi:10.1007/s11120-005-1440-4
6. Y. Umena, K. Kawakami, J.-R. Shen, N. Kamiya, Crystal structure of oxygen-evolving photosystem II at a resolution of 1.9 Å. *Nature* **473**, 55–60 (2011). Medline doi:10.1038/nature09913
7. W. A. Sidler, in *The Molecular Biology of Cyanobacteria*, vol. 1 of *Advances in Photosynthesis and Respiration*, D. A. Bryant, Ed. (Kluwer Academic, Dordrecht, Netherlands, 1994), pp. 139–216
8. Y. Fujita, A. Murakami, K. Aizawa, K. Ohki, in *The Molecular Biology of Cyanobacteria*, vol. 1 of *Advances in Photosynthesis and Respiration*, D. A. Bryant, Ed. (Kluwer Academic, Dordrecht, Netherlands, 1994), pp. 677–692.
9. C. Dong, A. Tang, J. Zhao, C. W. Mullineaux, G. Shen, D. A. Bryant, ApcD is necessary for efficient energy transfer from phycobilisomes to photosystem I and helps to prevent photoinhibition in the cyanobacterium *Synechococcus* sp. PCC 7002. *Biochim. Biophys. Acta* **1787**, 1122–1128 (2009). Medline doi:10.1016/j.bbabio.2009.04.007
10. H. Liu, H. Zhang, D. M. Niedzwiedzki, M. Prado, G. He, M. L. Gross, R. E. Blankenship, Phycobilisomes supply excitations to both photosystems in a megacomplex in cyanobacteria. *Science* **342**, 1104–1107 (2013). Medline doi:10.1126/science.1242321
11. D. Kirilovsky, C. A. Kerfeld, The orange carotenoid protein: A blue-green light photoactive protein. *Photochem. Photobiol. Sci.* **12**, 1135–1143 (2013). Medline doi:10.1039/c3pp25406b
12. M. Chen, R. E. Blankenship, Expanding the solar spectrum used by photosynthesis. *Trends Plant Sci.* **16**, 427–431 (2011). Medline doi:10.1016/j.tplants.2011.03.011
13. J. A. Maresca, J. E. Graham, D. A. Bryant, The biochemical basis for structural diversity in the carotenoids of chlorophototrophic bacteria. *Photosynth. Res.* **97**, 121–140 (2008). Medline doi:10.1007/s11120-008-9312-3
14. T. S. Bibby, J. Nield, J. Barber, Iron deficiency induces the formation of an antenna ring around trimeric photosystem I in cyanobacteria. *Nature* **412**, 743–745 (2001). Medline doi:10.1038/35089098
15. E. J. Boekema, A. Hifney, A. E. Yakushevska, M. Piotrowski, W. Keegstra, S. Berry, K. P. Michel, E. K. Pistorius, J. Kruip, A giant chlorophyll-protein complex induced by iron deficiency in cyanobacteria. *Nature* **412**, 745–748 (2001). Medline doi:10.1038/35089104
16. A. R. Grossman, M. R. Schaefer, G. G. Chiang, J. L. Collier, The phycobilisome, a light-harvesting complex responsive to environmental conditions. *Microbiol. Rev.* **57**, 725–749 (1993). Medline
17. N. Gaidukov, *Abh. Preuss. Akad. Wiss.* **5**, 1–36 (1902).
18. N. Gaidukov, *Ber. Dtsch. Bot. Ges.* **21**, 517–522 (1903).
19. D. M. Kehoe, A. Gutu, Responding to color: The regulation of complementary chromatic adaptation. *Annu. Rev. Plant Biol.* **57**, 127–150 (2006). Medline doi:10.1146/annurev.arplant.57.032905.105215
20. A. Gutu, D. M. Kehoe, Emerging perspectives on the mechanisms, regulation, and distribution of light color acclimation in cyanobacteria. *Mol. Plant* **5**, 1–13 (2012). Medline doi:10.1093/mp/ssr054
21. D. A. Bryant, G. Cohen-Bazire, Effects of chromatic illumination on cyanobacterial phycobilisomes: Evidence for the specific induction of a second pair of phycocyanin subunits in *Pseudanabaena* 7409 grown in red light. *Eur. J. Biochem.* **119**, 415–424 (1981). Medline doi:10.1111/j.1432-1033.1981.tb05624.x
22. D. A. Bryant, The photoregulated expression of multiple phycocyanin species:

A general mechanism for the control of phycocyanin synthesis in chromatically adapting cyanobacteria. *Eur. J. Biochem.* **119**, 425–429 (1981). Medline doi:10.1111/j.1432-1033.1981.tb05625.x
23. Y. Hirose, N. C. Rockwell, K. Nishiyama, R. Narikawa, Y. Ukaji, K. Inomata, J. C. Lagarias, M. Ikeuchi, Green/red cyanobacteriochromes regulate complementary chromatic acclimation via a protochromic photocycle. *Proc. Natl. Acad. Sci. U.S.A.* **110**, 4974–4979 (2013). Medline doi:10.1073/pnas.1302909110
24. I. I. Brown, D. A. Bryant, D. Casamatta, K. L. Thomas-Keprta, S. A. Sarkisova, G. Shen, J. E. Graham, E. S. Boyd, J. W. Peters, D. H. Garrison, D. S. McKay, Polyphasic characterization of a thermotolerant siderophilic filamentous cyanobacterium that produces intracellular iron deposits. *Appl. Environ. Microbiol.* **76**, 6664–6672 (2010). Medline doi:10.1128/AEM.00662-10
25. M. Chen, M. Schliep, R. D. Willows, Z. L. Cai, B. A. Neilan, H. Scheer, A red-shifted chlorophyll. *Science* **329**, 1318–1319 (2010). Medline doi:10.1126/science.1191127
26. M. Chen, Y. Li, D. Birch, R. D. Willows, A cyanobacterium that contains chlorophyll f—a red-absorbing photopigment. *FEBS Lett.* **586**, 3249–3254 (2012). Medline doi:10.1016/j.febslet.2012.06.045
27. R. Rippka, J. Deruelles, J. B. Waterbury, M. Herdman, R. Y. Stanier, Generic assignments, strain histories and properties of pure cultures of cyanobacteria. *J. Gen. Microbiol.* **111**, 1–61 (1979). doi:10.1099/00221287-111-1-1
28. Materials and methods are available as supplementary materials on *Science* Online.
29. N. C. Rockwell, Y. S. Su, J. C. Lagarias, Phytochrome structure and signaling mechanisms. *Annu. Rev. Plant Biol.* **57**, 837–858 (2006). Medline doi:10.1146/annurev.arplant.56.032604.144208
30. A. Biswas, Y. M. Vasquez, T. M. Dragomani, M. L. Kronfel, S. R. Williams, R. M. Alvey, D. A. Bryant, W. M. Schluchter, Biosynthesis of cyanobacterial phycobiliproteins in *Escherichia coli*: Chromophorylation efficiency and specificity of all bilin lyases from *Synechococcus* sp. strain PCC 7002. *Appl. Environ. Microbiol.* **76**, 2729–2739 (2010). Medline doi:10.1128/AEM.03100-09
31. N. C. Rockwell, J. C. Lagarias, A brief history of phytochromes. *ChemPhysChem* **11**, 1172–1180 (2010). Medline doi:10.1002/cphc.200900894
32. M. E. Auldridge, K. T. Forest, Bacterial phytochromes: More than meets the light. *Crit. Rev. Biochem. Mol. Biol.* **46**, 67–88 (2011). Medline doi:10.3109/10409238.2010.546389
33. Y. Li, N. Scales, R. E. Blankenship, R. D. Willows, M. Chen, Extinction coefficient for red-shifted chlorophylls: Chlorophyll *d* and chlorophyll *f*. *Biochim. Biophys. Acta* **1817**, 1292–1298 (2012). Medline doi:10.1016/j.bbabio.2012.02.026
34. Y. Li, Z.-L. Cai, M. Chen, Spectroscopic properties of chlorophyll *f*. *J. Phys. Chem. B* **117**, 11309–11317 (2013). Medline doi:10.1021/jp402413d
35. H. D. Christman, E. L. Campbell, J. C. Meeks, Global transcription profiles of the nitrogen stress response resulting in heterocyst or hormogonium development in *Nostoc punctiforme*. *J. Bacteriol.* **193**, 6874–6886 (2011). Medline doi:10.1128/JB.05999-11
36. A. N. Glazer, D. A. Bryant, Allophycocyanin B (lambdamax 671, 618 nm): A new cyanobacterial phycobiliprotein. *Arch. Microbiol.* **104**, 15–22 (1975). Medline doi:10.1007/BF00447294
37. R. M. Alvey, A. Biswas, W. M. Schluchter, D. A. Bryant, Attachment of noncognate chromophores to CpcA of *Synechocystis* sp. PCC 6803 and *Synechococcus* sp. PCC 7002 by heterologous expression in *Escherichia coli*. *Biochemistry* **50**, 4890–4902 (2011). Medline doi:10.1021/bi200307s
38. A. Ducret, S. A. Müller, K. N. Goldie, A. Hefti, W. A. Sidler, H. Zuber, A. Engel, Reconstitution, characterisation and mass analysis of the pentacylindrical allophycocyanin core complex from the cyanobacterium *Anabaena* sp. PCC 7120. *J. Mol. Biol.* **278**, 369–388 (1998). Medline doi:10.1006/jmbi.1998.1678
39. Y. M. Gindt, J. Zhou, D. A. Bryant, K. Sauer, Spectroscopic studies of phycobilisome subcore preparations lacking key core chromophores: Assignment of excited state energies to the Lcm, beta 18 and alpha AP-B chromophores. *Biochim. Biophys. Acta* **1186**, 153–162 (1994). Medline doi:10.1016/0005-2728(94)90174-0
40. P. Mulo, I. Sakurai, E.-M. Aro, Strategies for psbA gene expression in cyanobacteria, green algae and higher plants: From transcription to PSII repair. *Biochim. Biophys. Acta* **1817**, 247–257 (2012). Medline doi:10.1016/j.bbabio.2011.04.011
41. E. Kiss, P. B. Kós, M. Chen, I. Vass, A unique regulation of the expression of the psbA, psbD, and psbE genes, encoding the 01, 02 and cytochrome b559 subunits of the Photosystem II complex in the chlorophyll d containing cyanobacterium *Acaryochloris marina*. *Biochim. Biophys. Acta* **1817**, 1083–1094 (2012). Medline doi:10.1016/j.bbabio.2012.04.010
42. M. Tester, C. Morris, The penetration of light through soil. *Plant Cell Environ.* **10**, 281–286 (1987). doi:10.1111/j.1365-3040.1987.tb01607.x
43. D. Bliss, H. Smith, Penetration of light into soil and its role in the control of seed germination. *Plant Cell Environ.* **8**, 475–483 (1985). doi:10.1111/j.1365-3040.1985.tb01683.x
44. D. A. Bryant, Z. Liu, in *Genome Evolution of Photosynthetic Bacteria*, J. T. Beatty, Ed., vol. 66 of *Advances in Botanical Research* (Elsevier, New York, 2013), pp. 99–150.
45. J. F. Allen, W. Martin, Evolutionary biology: Out of thin air. *Nature* **445**, 610–612 (2007). Medline doi:10.1038/445610a
46. F. L. Sousa, L. Shavit-Grievink, J. F. Allen, W. F. Martin, Chlorophyll biosynthesis gene evolution indicates photosystem gene duplication, not photosystem merger, at the origin of oxygenic photosynthesis. *Genome Biol. Evol.* **5**, 200–216 (2013). Medline doi:10.1093/gbe/evs127
47. P. Jordan, P. Fromme, H. T. Witt, O. Klukas, W. Saenger, N. Krauß, Three-dimensional structure of cyanobacterial photosystem I at 2.5 A resolution. *Nature* **411**, 909–917 (2001). Medline doi:10.1038/35082000
48. A. Guskov, J. Kern, A. Gabdulkhakov, M. Broser, A. Zouni, W. Saenger, Cyanobacterial photosystem II at 2.9-Å resolution and the role of quinones, lipids, channels and chloride. *Nat. Struct. Mol. Biol.* **16**, 334–342 (2009). Medline doi:10.1038/nsmb.1559
49. S. Q. Le, O. Gascuel, Accounting for solvent accessibility and secondary structure in protein *phylogenetics* is clearly beneficial. *Syst. Biol.* **59**, 277–287 (2010). Medline doi:10.1093/sysbio/syq002
50. K. C. Yeh, S. H. Wu, J. T. Murphy, J. C. Lagarias, A cyanobacterial phytochrome two-*component* light sensory system. *Science* **277**, 1505–1508 (1997). Medline doi:10.1126/science.277.5331.1505
51. L. O. Essen, J. Mailliet, J. *Hughes*, The structure of a complete phytochrome sensory module in the Pr ground state. *Proc. Natl. Acad. Sci. U.S.A.* **105**, 14709–14714 (2008). Medline doi:10.1073/pnas.0806477105
52. K. Anders, G. Daminelli-Widany, M. A. Mroginski, D. von Stetten, L. O. Essen, Structure of *the* cyanobacterial phytochrome 2 photosensor implies a tryptophan switch for phytochrome signaling. *J. Biol. Chem.* **288**, 35714–35725 (2013). Medline doi:10.1074/jbc.M113.510461
53. R. C. Edgar, MUSCLE: *Multiple* sequence alignment with high accuracy and high throughput. *Nucleic Acids Res.* **32**, 1792–1797 (2004). Medline doi:10.1093/nar/gkh340
54. N. C. Rockwell, L. Shang, S. S. Martin, J. C. Lagarias, Distinct classes of red/far-red photochemistry within the phytochrome superfamily. *Proc. Natl. Acad. Sci. U.S.A.* **106**, 6123–6127 (2009). Medline doi:10.1073/pnas.0902370106
55. M. Ludwig, D. A. Bryant, Transcription profiling of the model cyanobacterium Synechococcus sp. strain PCC 7002 by Next-Gen (SOLiD™) sequencing of cDNA. *Front. Microbiol.* **2**, 41 (2011). Medline doi:10.3389/fmicb.2011.00041
56. H. Li, R. Durbin, Fast and accurate short read alignment with Burrows-Wheeler transform. *Bioinformatics* **25**, 1754–1760 (2009). Medline doi:10.1093/bioinformatics/btp324
57. I. V. Shilov, S. L. Seymour, A. A. Patel, A. Loboda, W. H. Tang, S. P. Keating, C. L. Hunter, L. M. Nuwaysir, D. A. Schaeffer, The Paragon algorithm, a next generation search engine that uses sequence temperature values and feature probabilities to identify peptides from tandem mass spectra. *Mol. Cell. Proteomics* **6**, 1638–1655 (2007). Medline doi:10.1074/mcp.T600050-MCP200
58. C. T. Nomura, S. Persson, G. Shen, K. Inoue-Sakamoto, D. A. Bryant, Characterization of two cytochrome oxidase operons in the marine cyanobacterium *Synechococcus* sp. PCC 7002: inactivation of ctaDI affects the PS I:PS II ratio. *Photosynth. Res.* **87**, 215–228 (2006). Medline doi:10.1007/s11120-005-8533-y
59. Y. Li, Y. Lin, P. C. Loughlin, M. Chen, Optimization and effects of different culture conditions on growth of *Halomicronema hongdechloris* - a filamentous cyanobacterium containing chlorophyll *f*. *Front. Plant Sci.* **5**, 67

(2014). Medline doi:10.3389/fpls.2014.00067
60. R. M. Alvey, A. Biswas, W. M. Schluchter, D. A. Bryant, Effects of modified phycobilin biosynthesis in the cyanobacterium *Synechococcus* sp. strain PCC 7002. *J. Bacteriol.* **193**, 1663–1671 (2011). Medline doi:10.1128/JB.01392-10

ACKNOWLEDGMENTS

This study was funded by grant MCB-1021725 from the National Science Foundation to D.A.B. The genome sequence of *Leptolyngbya* sp. strain JSC-1 was determined under the auspices of the U.S. Department of Energy's Office of Science, Biological and Environmental Research Program, and by the University of California, Lawrence Berkeley National Laboratory under contract no. DE-AC02-05CH11231, Lawrence Livermore National Laboratory under contract no. DE-AC52-07NA27344, and Los Alamos National Laboratory under contract no. DE-AC02-06NA25396. Spectroscopic characterization of RfpA and NpR4776-PCM was funded by a grant from the Chemical Sciences, Geosciences, and Biosciences Division, Office of Basic Energy Sciences, Office of Science, U.S. Department of Energy (DOE DE-FG02-09ER16117 to J.C.L.) The authors thank James R. Miller for assistance in performing mass analyses on Chls *d* and *f;* Bruce Stanley and Anne Stanley for advice and technical assistance in performing the tryptic peptide mass fingerprinting; and Craig Praul and Candace Price for assistance in performing RNA-Seq profiling. The authors thank Juliette Lecomte, Wendy Schluchter, John Golbeck, and Alexander Glazer for reading the manuscript and helpful suggestions. This Whole-Genome Shotgun project for *Leptolyngbya* sp. strain JSC-1 (alternative name, *Marsacia ferruginose*; IMG taxon ID 2022827000; GOLD ID = Gi02032) has been deposited at DDBJ/EMBL/GenBank under the accession JMKF00000000; the version described in this paper is version JMKF01000000. RNA-Seq data were deposited in the NCBI Sequence Read Archive (SRA) under accession number SRP041154.

SUPPLEMENTARY MATERIALS

www.sciencemag.org/cgi/content/full/science.1256963/DC1
Materials and Methods
Figs. S1 to S18
Tables S1 and S2
References (*49–60*)

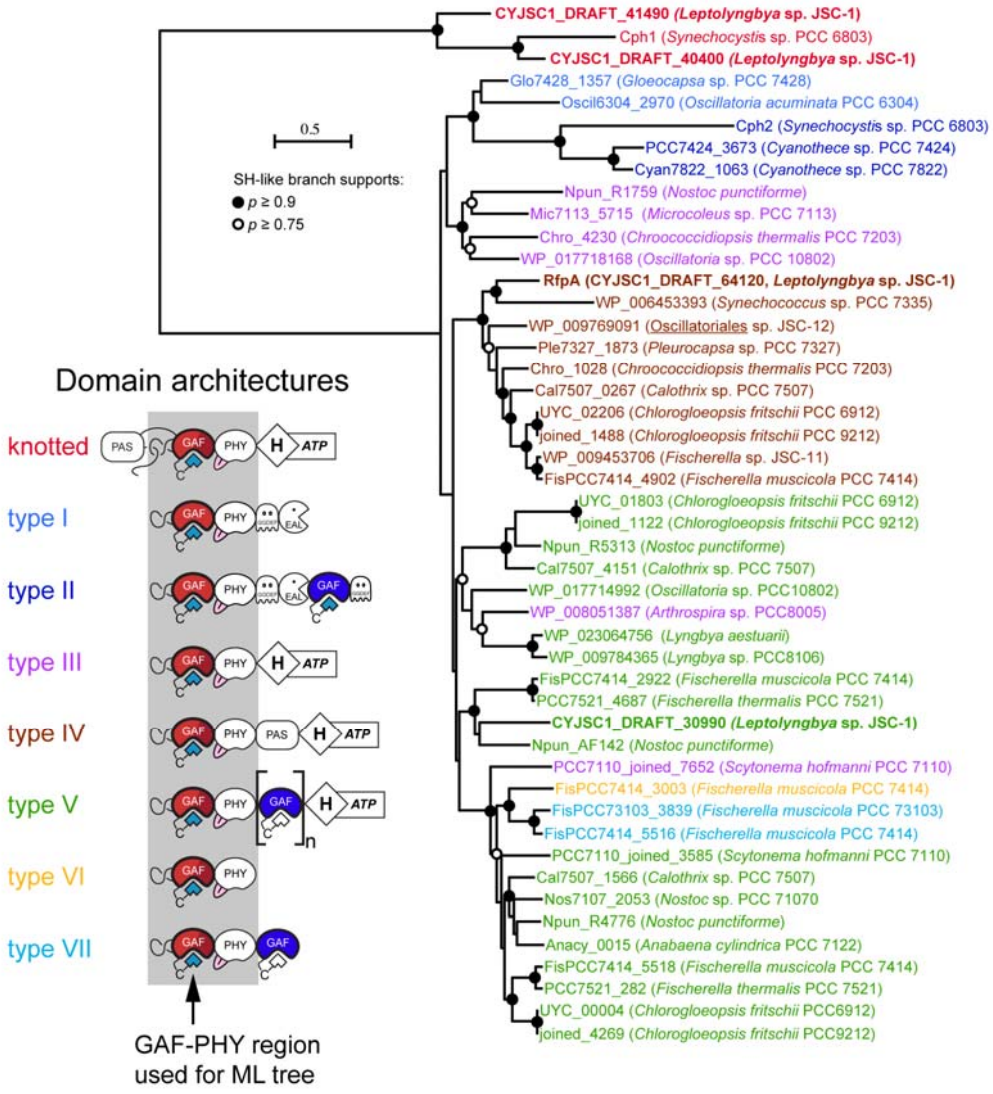

Fig. 1. RfpA forms a distinctive lineage of knotless phytochromes. The GAF-PHY domains of selected knotless phytochromes, including the products of ten *rfpA* genes (fig. S3), were aligned with *Synechocystis* sp. PCC 6803 Cph1 and two closely related, knotted phytochromes from *Leptolyngbya* sp. JSC-1 as an outgroup (fig. S4). The resulting alignment was used to produce a maximum likelihood phylogenetic tree; open and closed circles at nodes show the approximate statistical support for the branching pattern as indicated. The colors of the sequence names reflect seven domain architectures for knotless phytochromes (lower left), with phytochrome and related photosensory GAF domains highlighted in red and blue, respectively. RfpA orthologs have a conserved domain architecture (type IV) and form a distinct subfamily of knotless phytochromes, providing two independent lines of evidence that RfpA orthologs form a distinct lineage associated with FarLiP gene clusters (fig. S3).

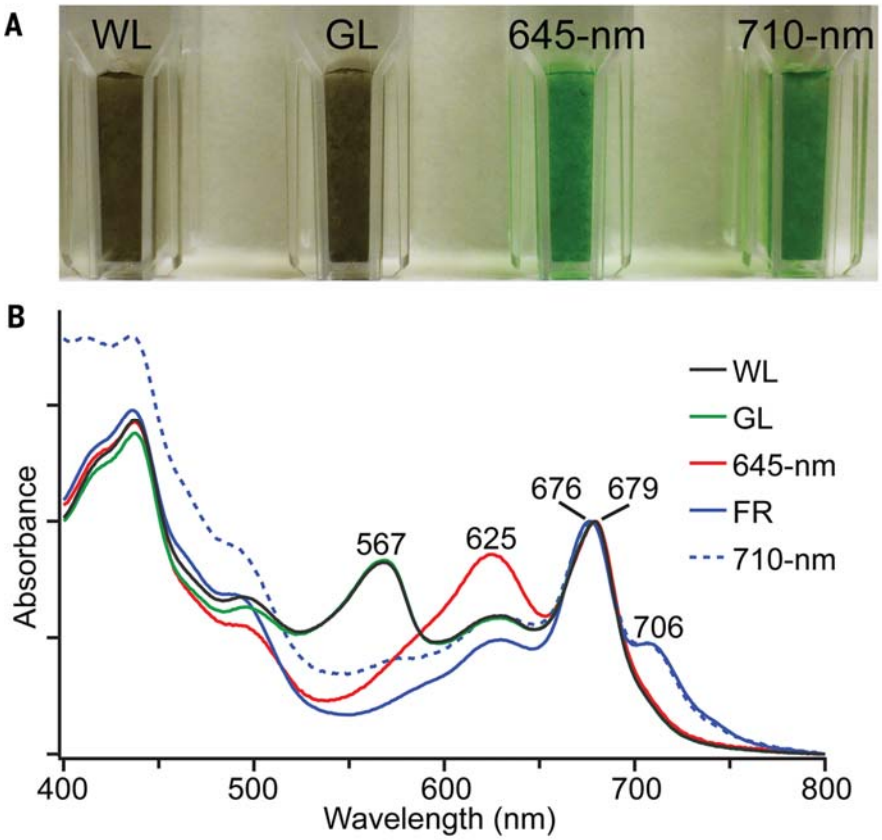

Fig. 2. JSC-1 cells have enhanced absorption at 700 to 750 nm when grown in far-red light. (**A**). Appearance of cells grown in WL, GL, 645-nm light and 710-nm light. (**B**) Absorption spectra of strain JSC-1 cells grown in WL (black line), GL (green line), 645-nm light (red line), FR (solid blue line) and 710-nm light (dotted blue line).

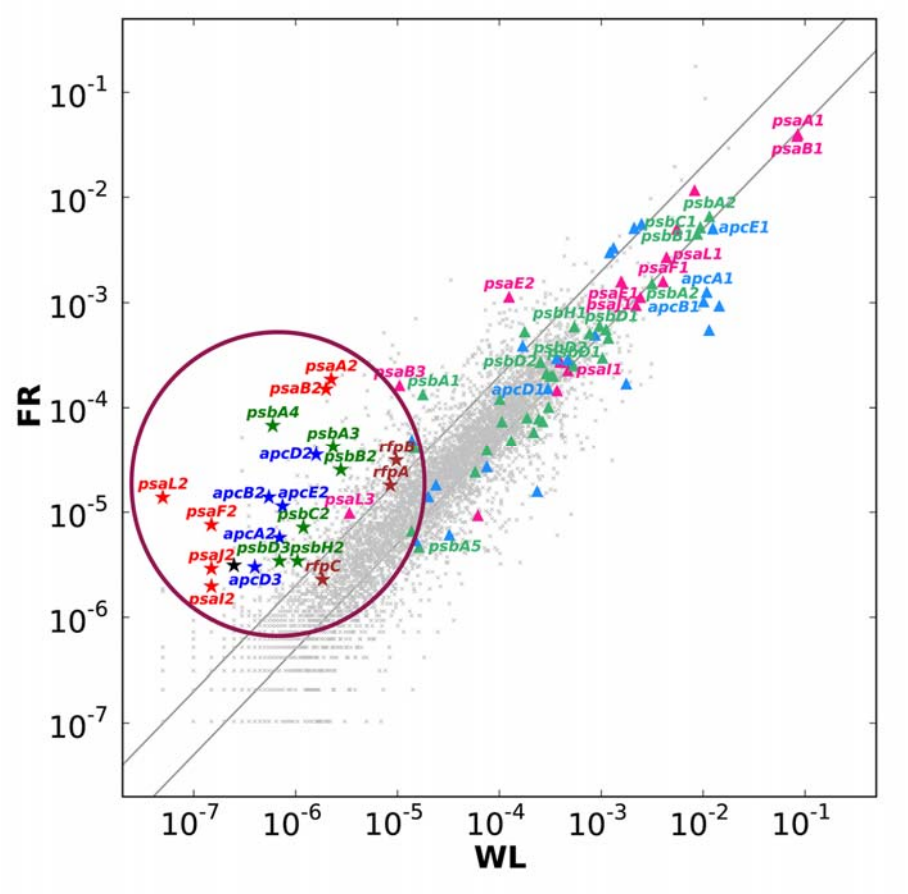

Fig. 3. Transcription of the 21-gene cluster in JSC-1 in far-red light is part of an extensive acclimative response. Scatter plot showing relative transcript levels for JSC-1 cells 24 hours after a shift from WL to FR. The circled stars indicate the relative transcript levels for the genes in the 21-gene cluster shown in fig. S2. The magenta, pale green and aqua triangles indicate relative transcript levels for paralogous genes encoding subunits of PS I, PS II, and PBS, respectively, that are preferentially expressed in WL. The parallel lines indicate a 2-fold increase or decrease in transcript abundance.

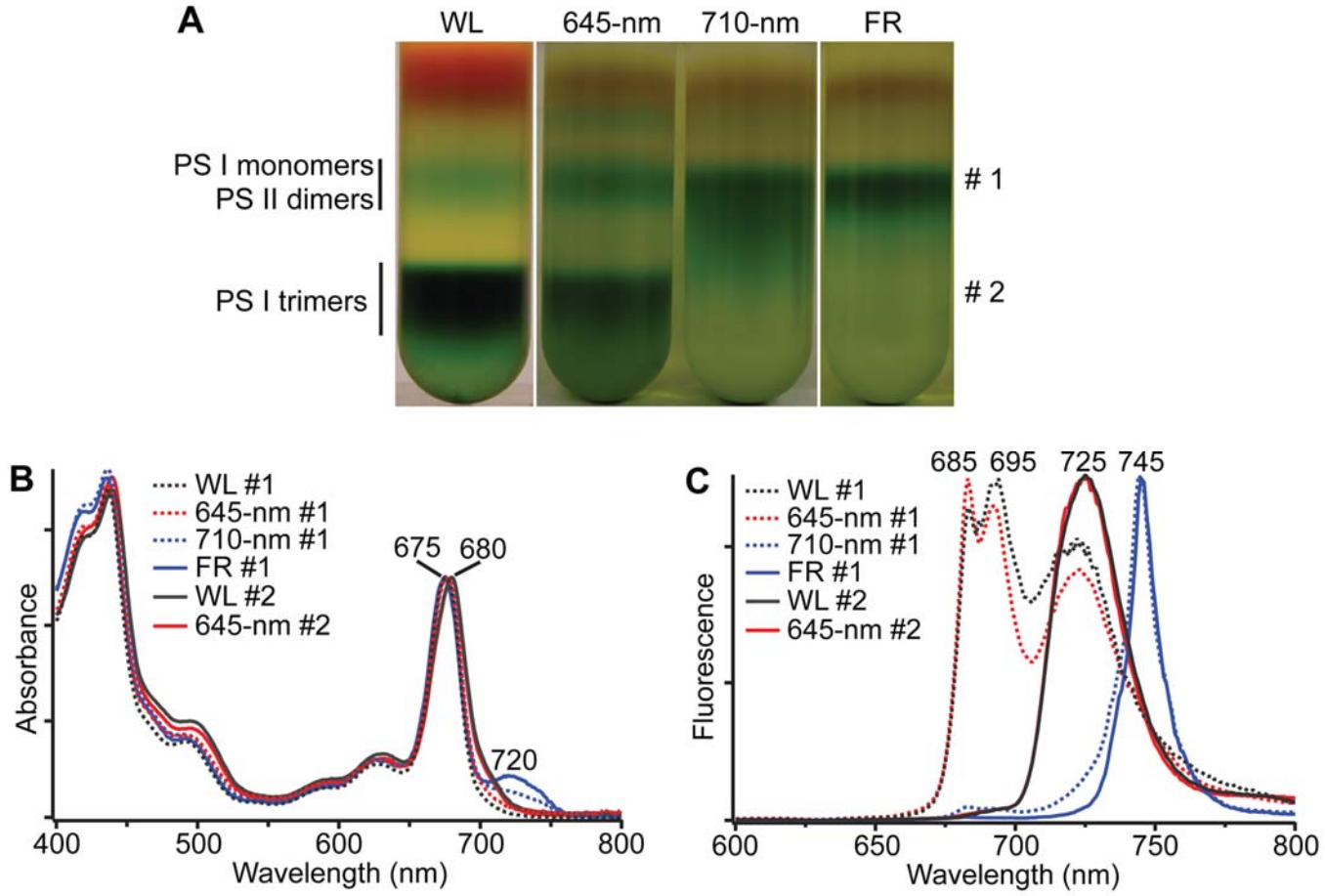

Fig. 4. PS I and PS II complexes are remodeled under far-red light. (**A**) Sucrose density gradient centrifugation for isolation of Chl-containing complexes from thylakoid membranes of JSC-1 cells grown in WL, 645-nm light, 710-nm light, and FR after solubilization with β-D-dodecylmaltoside. (**B**) Absorption spectra of gradient fractions containing PS I trimers (WL, solid black line; 645-nm light, solid red line) and a mixture of PS I monomers and PS II from WL (dashed black line); 645-nm light (dashed red line); FR (solid blue line); and 710-nm light (dashed blue line). (**C**). Low-temperature fluorescence emission spectra for the same fractions as in (B).

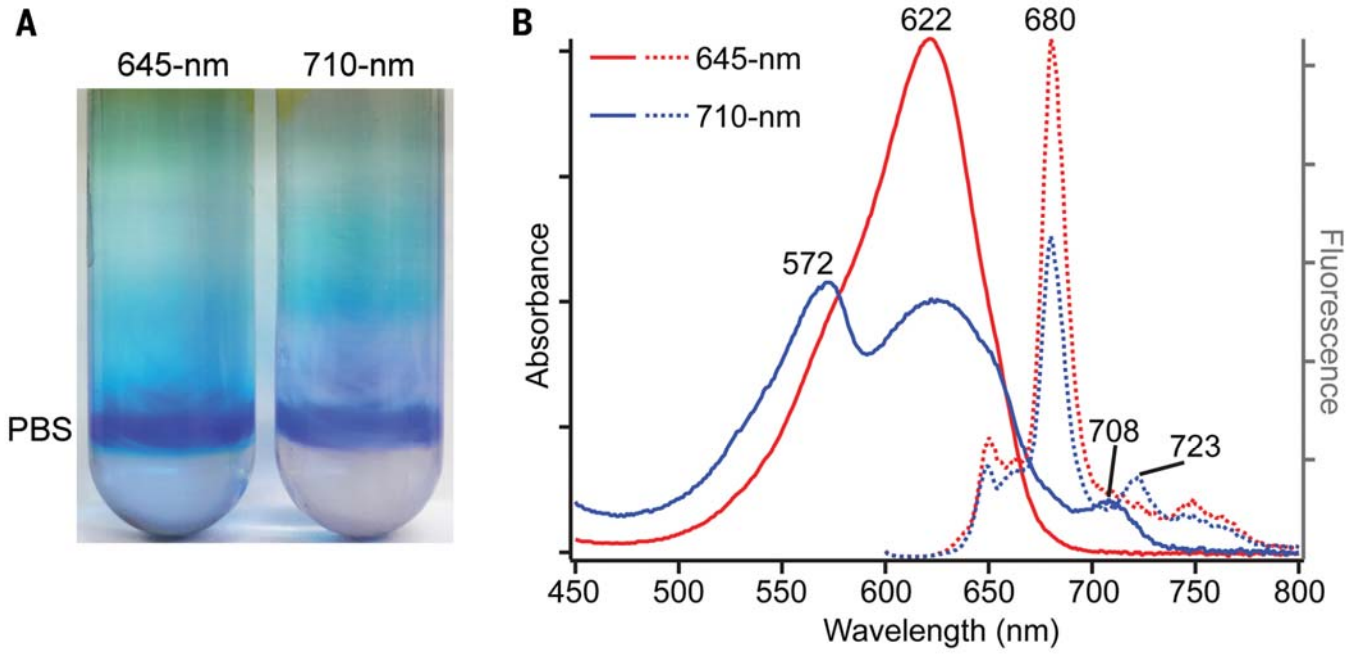

Fig. 5. Phycobilisomes isolated from cells grown in far-red light have enhanced absorption from 700 to 750 nm. (**A**) Sucrose gradients showing phycobilisomes isolated from cells grown in 645-nm light and 710-nm light. (**B**) Absorption spectra (solid lines) and fluorescence emission spectra (dashed lines) for PBS fractions from cells grown in 645-nm light (red lines) and 710-nm light (blue lines).

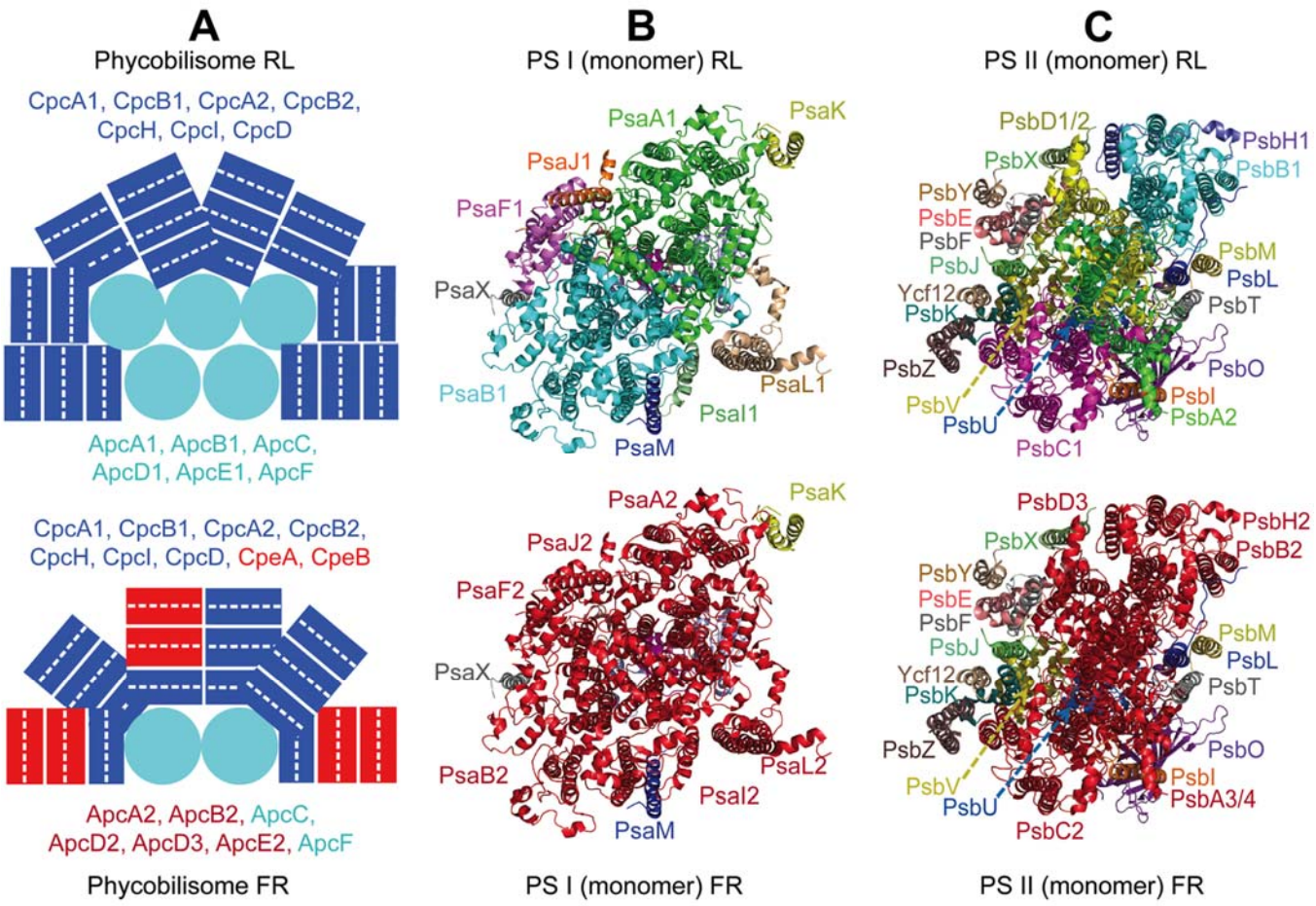

Fig. 6. Diagrams summarizing the remodeling of components of PBS, PS I, and PS II, during FaRLiP. (**A**) Remodeling of PBS cores in FR. Except ApcF and ApcC (see table S1), all allophycocyanin-related components (shown in aqua) comprising the PBS core substructure are replaced in FR. ApcE1 has four REP (linker) domains and should assemble a pentacylindrical substructure in cells grown in WL, GL, or RL (upper model). ApcE2 has only two REP (linker) domains and should assemble a bicylindrical core substructure in FR (*7*, *38*) (lower model). PBS assembled in FR contain some phycoerythrin (table S1; shown as red disks; phycocyanin is shown in blue). This may occur because FR cannot efficiently photoconvert the CCA photoreceptor into its green-absorbing (P_g form) (*23*). Remodeling of PS I (**B**) and PS II (**C**) illustrated using the X-ray structures of PS I (PDB = 1JB0) (*47*) and PS II (PDB = 3BZ2) (*48*) from *Thermosynechococcus elongatus*. The view of PS I is from the lumenal side, so PsaC, PsaD, and PsaE are not visible. The view of PS II is from the cytoplasm-facing side. Each subunit is shown in a different color in the upper structures, and subunits replaced in FR are shown in red in the lower structures. Subunit Ycf12 of PS II is not encoded in the draft genome of JSC-1.